Int. J. Multiphase Flow Vol. 4, pp. 237–262

0301-9322/78/0601-0237/$02.00/0

THE DYNAMICS AND DISSOLUTION OF GAS BUBBLES IN A VISCOELASTIC FLUID

E. ZANA† and L. G. LEAL

Chemical Engineering, California Institute of Technology, Pasadena, CA 91125, U.S.A.

(*Received* 14 *October* 1977)

Abstract—This paper reports an experimental study of the motion of dissolving and non-dissolving gas bubbles in a quiescent viscoelastic fluid. The objective of the investigation was to determine the influence of the abrupt transition in bubble velocity, which had been observed at a critical radius of approx. 0.3 cm, on the rate of mass transfer. Thus, a range of bubble sizes from an equivalent (spherical) radius of 0.2–0.4 cm was employed using CO_2 gas, and five different fluids, including one Newtonion glycerine/water solution and four viscoelastic solutions of Separan AP30 in water (0.1, 0.5, 1% by weight) and in a water/glycerine mixture.

The experimental data on bubble velocity shows that the discontinuous increase with bubble volume observed previously for air bubbles in viscoelastic fluids, does *not* occur for dissolving CO_2 bubbles—presumably due to the continuous decrease in bubble volume. Instead, a very steep but definitely continuous transition is found. Mass transfer rates are found to be significantly enhanced by viscoelasticity, and comparison with available theoretical results shows that the increase is greater than expected for purely viscous, power-law fluids. We conclude that a fully viscoelastic constitutive model would be necessary for a successful analysis of the dissolution of a gas bubble which is translating through a (high molecular weight) polymer solution.

A. INTRODUCTION

One of the most important problems of non-Newtonian fluid dynamics is the buoyancy-driven translational motion of gas bubbles through viscoelastic materials such as polymer solutions and melts. From the technolgical point of view, of particular interest is the application of the basic physical principles to the design and operation of gas–liquid contact mass-transfer equipment. However, even from a purely fundamental point of view, the motion of a single gas bubble is interesting as an example of a strongly non-viscometric flow which exhibits major macroscopic differences from its Newtonian counterpart. A detailed investigation of such problems is important to the gradual build-up of basic understanding of the mechanics of fully viscoelastic fluids.

Among the various phenomena which are exhibited by a gas bubble in a viscoelastic fluid perhaps the most striking is the existence of an abrupt (discontinuous) transition in terminal velocity of the bubble when measured as a function of the bubble volume. This transition was first reported by Astarita & Apuzzo (1965), who found a sixfold increase in bubble velocity at the critical bubble volume for a 0.5% solution of the commercial J-100 polymer. Similar results have more recently been reported by Calderbank *et al.* (1970) in 1% Polyox solutions and by Leal *et al.* (1971) in solutions of the commercial polymer, Separan AP30.

Most investigators who have studied the problem agree that the basic cause of the change in bubble velocity is a transition in conditions at the bubble surface from no-slip to a free (zero shear stress) surface regime, as was first suggested by Astarita & Apuzzo (1965). This transition is equivalent to the well-known change from the Stokes to Hadamard regime in a Newtonian liquid, and so, in itself, is not too surprising. Indeed, Leal *et al.* (1971) showed experimentally that bubble velocities for volumes less than the critical volume are precisely equal to those measured for equal volume glass spheres provided suitable density corrections are made. Furthermore, the glass spheres showed *no* transition in terminal velocity. Taken

†Present address: Chevron Oil Field Research, LaHabra, CA

together, these observations provide strong indirect evidence to support the contention that a change in surface conditions is responsible for the observed velocity transition in the case of gas bubbles. In contrast, however, it is *not* yet clear why the boundary-condition transition should occur so abruptly in the viscoelastic case, or for such large bubbles ($r_e \sim 0.3$ cm), when the Newtonian transition is known to occur for much smaller bubbles and smoothly as a function of bubble size. Furthermore, the magnitude of the change in terminal velocities is much bigger (as much as a factor of 6 or 10) in the viscoelastic case than in the Newtonian case (where the ratio at equal volumes is known theoretically to be approx. 3/2 for nearly spherical shapes) and no satisfactory explanation has yet been offered for this fact either. Astarita & Apuzzo (1965) did suggest correctly (in our view) that the magnitude of the transition was probably due, in some way, to the viscoelastic nature of the suspending fluid. However, Astarita & Apuzzo's further suggestion that the magnitude could actually be explained by considering only purely-viscous, shear-thinning effects (i.e. neglecting elasticity or normal stresses) was shown to be incorrect by Leal *et al.* (1971) who studied the effect of shear-dependent viscosity, in the absence of viscoelastic effects, using numerical methods with an empirical, purely-viscous fluid model. Calculations of the terminal velocities for non-circulating, partially circulating, and fully circulating spherical bubbles at the measured critical volume showed that shear-thinning alone could not possibly account for more than 30% of the measured magnitude of the velocity transition. However, it was also shown, by simple qualitative arguments, that a relatively *small* effect of *elasticity* on the bubble drag could be sufficient to account for the much larger measured velocity increase, *if* the drag were *reduced* by elastic effects in both the pre- and post-transition regimes, but with a somewhat greater reduction in the latter case.

An initial test of the viability of this latter argument was made by the present authors (see Zana 1975; Leal & Zana 1974) using "slow-flow" asymptotic solutions, based on the 6-constant Oldroyd (1958) fluid model, to compare the viscoelastic contributions to the drag on a rigid no-slip sphere and on a freely circulating spherical bubble of the same volume. The rigid sphere result was taken from Leslie (1961). The solution for the case of a spherical bubble was obtained by Zana (1975). In the limit corresponding to a *constant* shear viscosity it was shown that the drag is increased in both cases compared to the Newtonian value at second order, $0(We^2)$, in the retarded motion expansion. Significantly, however, the decrease is much more pronounced for the bubble than for the rigid, no-slip sphere. Thus, the "slow flow" viscoelastic approximation offers strong preliminary evidence to support the proposition of Leal *et al.* (1971).

From a more fundamental viewpoint, the problem of explaining the magnitude of the velocity transition requires a mechanism to account for much stronger influence of the surface boundary conditions with viscoelastic fluids, as compared to Newtonian fluids where the terminal velocity ratio is approx. 3/2. We believe that the answer must lie in the fundamentally different types of flow generated near a bubble and near a rigid sphere. In the latter case, the no-slip condition causes the local disturbance flow near the sphere to be largely a simple shear flow, subject to shear thinning. For the bubble, however, the surface is free, and the local disturbance flow is then dominated by extensional and compressional deformations. To relate these observations to a quantitative discussion of the magnitude of the transition, further theoretical effort is necessary to obtain (numerical) solutions for the flow past spherical bodies which are not restricted to "slow" (nearly Newtonian) flows.

The primary objective of the present work is more nearly an assessment of the technological significance of the transition, than an attempt to provide any further explanation of its existence or its form. In particular, we will consider the mass transfer characteristics of a single bubble in the transition regime. With the exception of one data set for CO_2 in a 1.0% solution of Polyox in water by Calderbank *et al.* (1970), no attention has yet been given to the influence of the velocity transition on mass transfer. Indeed, very little work has apparently been done on bubble mass-transfer in viscoelastic fluids for *any* regime. In the present investigation, we

report experimentally determined rates of mass transfer for single gas bubbles in a viscoelastic liquid. In order to assist in data interpretation, we have also repeated some of the earlier measurements of shape and terminal velocity, with particular emphasis on the differences between dissolving and non-dissolving bubbles. The terminal velocity behavior does provide some further insight into the abruptness of the velocity transition which was reported in earlier studies. In addition to providing a more extensive correlation of mass transfer rates and rheological properties of the suspending fluid, the present study also differs fundamentally from the earlier work of Calderbank (1970) in the method of measurement. In Calderbank's work the bubble volume is held constant and the internal gas concentration goes down, while in the present work the bubble volume changes freely as the mass transfer process proceeds.

B. DIMENIONAL ANALYSIS AND THEORETICAL BACKGROUND

An important initial step in the design and interpretation of the mass-transfer experiments is a determination of the physical and rheological parameters which will play a fundamental role in the bubble dynamics and mass-transfer processes. This is most easily accomplished by dimensional analysis based on the governing differential equations and boundary conditions. It is convenient to begin by considering the purely dynamical problem of a bubble of constant volume translating with a fixed velocity through a viscoelastic fluid. For present purposes, the precise form of the constitutive model is not critical. The natural characteristic variables for non-dimensionalization are the radius of a sphere with the same volume as the bubble (which may be deformed), R_{eq}, the steady, terminal velocity of translation, U_∞, and the characteristic stress, $\mu U_\infty/R_{eq}$. With these choices, the parameters which appear in the dimensionless equations of motion and continuity are the Reynolds number, $Re \equiv 2R_{eq}U_\infty/\nu$; the Weissenberg number based on the principal relaxation time of the fluid, $We \equiv U_\infty\lambda_1/R_{eq}$; and a series of ratios of the intrinsic time constants of the constitutive model. Although Re and We can vary widely ($0 < Re < \infty$, $0 < We < \infty$), these ratios of dimensionless time constants are generally of order unity and vary relatively little from fluid to fluid. This means that any qualitative discussion of bubble dynamics in a viscoelastic fluid can focus on the magnitudes of the Reynolds number and the Weissenberg number plus any additional parameters which may appear in the boundary conditions. In the simplest circumstances, it is only the surface tension which is important, and then only as a parameter which controls bubble shape. While the details of motion are certainly influenced by the shape, the main features of viscoelastic flow past a bubble are determined by the nature of the fluid and are the same for any shape which is not too far removed from spherical. For purposes of the present discussion, it is thus convenient to consider the roles of inertia, viscous and "elastic" forces for a bubble of fixed (spherical) shape.

In general terms, the Reynolds number is a measure of the ratio of inertia to viscous forces, the Weissenberg number a measure of the ratio of elastic to viscous forces, and We/Re a measure of the ratio of elastic to inertia forces. Several distinct regimes are thus possible, depending upon the relative magnitudes of Re and We. For low Reynolds number, the flow characteristics are determined by a balance between elastic and viscous/pressure forces. In this regime, the important parameter is thus We and the rheological properties of the suspending fluid generally play a significant role. However, as the bubble volume is *decreased*, U decreases (in every case known to us) at a rate proportional to R_{eq}^m with $m > 1$. Thus, in such cases the Weissenberg number, $We \to 0$, and the purely viscous effects eventually dominate the dynamics for sufficiently small bubbles. The fluid motion in this regime is then expected to be identical with that in a Newtonian fluid with equivalent viscosity. As the bubble volume is *increased* elastic contributions become more important; however, so do inertia effects, and the important parameter is We/Re. Eventually, for even larger bubbles, $We/Re \to 0$, and the fluid motion is dominated by inertia effects *everywhere* in the flow domain. This is quite different from the case of high Reynolds number flow past a solid body where the viscous and elastic effects always remain important in a thin layer near the body, and is a consequence of the surface boundary

conditions which require zero tangential stress rather than zero tangential velocity. In this inertia dominated regime the flow characteristics are expected to be completely independent of the fluid rheology.

Let us now return, briefly, to the bubble shape. In general, the bubble will be more or less deformed from a sphere depending upon the relative magnitude of inertia or elastic forces and the tensile surface forces. At small *Re*, it is the elastic forces balanced with surface forces which determine the shape, and we conclude that the parameter

$$\frac{\mu U_\infty}{\sigma} We \equiv \left(\frac{Wb}{Re}\right) We$$

is important. Here, *Wb* is the Weber number, defined as $Wb \equiv \rho R_{eq} U_\infty^2/\sigma$. On the other hand, at large *Re*, it is the inertia/surface force balance which determines the bubble shape, and thus *Wb* alone is the significant independent parameter. In the latter case, the bubble shape is expected to be completely independent of the rheological properties of the suspending fluid.

We have suggested that the fluid dynamical effects of viscoelasticity can be mainly accounted for by consideration of the magnitude of the *Re* and *We* numbers. One difficulty with this approach is that none of the generally accepted constitutive models for viscoelastic liquids is capable of modelling purely-viscous fluids (such as CMC solutions) which exhibit strong shear thinning, but no other measurable manifestation of viscoelasticity. In general, to reduce elastic effects we would naturally consider the limit $We \to 0$, but in existing models this has the simultaneous effect of reducing the degree of shear-thinning. It is thus necessary to have some alternative means of specifying the degree of shear-thinning independently of the magnitude of elastic effects. A convenient, if *ad hoc*, approach is to use a simple power-law model

$$\tau = -\left\{m\left|\frac{1}{2}\mathbf{e}:\mathbf{e}\right|^{(n-1)/2}\right\}\mathbf{e}$$

to provide a second rheological parameter, *n*, which is capable of reflecting the degree of shear-thinning independently from the degree of elasticity as measured by *We*.

In the presence of mass transfer, the equations of motion and continuity must be supplemented by the convective-diffusion equation for the dissolving material. Coupling between the fluid dynamics and the mass transfer process occurs in at least three ways. First, the velocity field enters directly into the convection terms in the convective-diffusion equation. Second, since material is being transferred either from or to the bubble, its volume will change, thus inducing a time dependent normal velocity in the vicinity of the bubble surface. Third, as the bubble volume changes, both the buoyancy force and the bubble velocity will vary continuously with time. All of these effects must be taken into account in any general analysis of the bubble mass transfer process.

If a characteristic time, R_{eq}^2/D, is used to define a dimensionless time scale $\bar{t} = t/(R_{eq}^2/D)$, and the time-dependent govering equations are again nondimensionalized, one new parameter enters the system, namely, the Peclet number, $Pe \equiv U_\infty R_{eq}/D$. The Peclet number is a measure of the relative magnitude of the convection terms compared with diffusion and time-dependent terms in the convective-diffusion equation. The characteristic time R_{eq}^2/D, is chosen since the time-dependence of the bubble motion is completely due to the diffusion-induced change in the bubble volume. *Peclet number may thus be seen to also provide a measure of the instantaneous velocity of rise of the bubble compared to the normal velocity induced at the bubble surface by its change in volume.* Depending on the magnitude of the Peclet number, two distinct limiting cases can be identified.

When Peclet number is large ($Pe \gg 1$), the velocity field is dominated by the free streaming motion which is due to the buoyancy-driven bubble rise. The induced velocity due to bubble

collapse is, in this limit, asymptotically small. Thus to a first approximation, the equations of motion and continuity may be solved without consideration of the mass-transfer process. The only effect of the fluid rheology on mass transfer is an indirect result of its effect on the velocity field which must be used to evaluate the convection terms in the convective-diffusion equation.

For small values of the Peclet number the velocity field is dominated by the motion induced by the bubble collapse, and the mass-transfer problem reduces at first order to the dissolution of a stationary gas bubble in a quiescent, viscoelastic fluid. In this case, the viscoelastic properties of the fluid are of direct significance. Indeed, the high stresses, which occur in a viscoelastic fluid as a result of the extensional motions which are induced by the bubble collapse, can inhibit the collapse rates to such an extent that the whole mass-transfer process is controlled by the fluid rheology.

In an earlier paper, Zana & Leal (1975) we analyzed the dependence of mass-transfer rate on the rheological properties of the suspending fluid in some detail for the latter case $Pe \ll 1$. The present experimental work is mainly concerned with the opposite limit, $Pe \gg 1$, for bubble volumes which are initially near to the critical size for the velocity transition phenomenon.

C. EXPERIMENTAL METHODS

1. *Description of the apparatus*

A schematic diagram of the apparatus used in the experiments is shown in figure 1. The main features are a pair of humidifying columns and an airtight test (absorption) column, a motor-driven camera platform with associated controls and lighting, a specially designed bubble release mechanism, and a pressure measuring system with associated electronics and controls. Of these features, all were used extensively in the present study except for the pressure system which is primarily intended for mass-transfer measurements in less viscous fluids where the bubble shape is not steady (see section C3). The purpose of the humidifying columns is to saturate the gas bubble with water vapor before it is introduced into the absorption column. The actual test (absorption) column is constructed of 1/2 to 3/4 inch Plexiglas sheet and is seven feet in height with a six-inch square cross section.

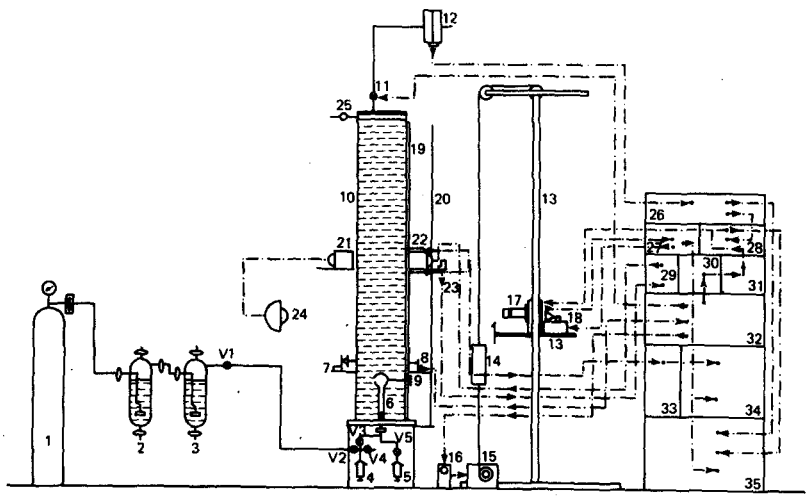

Figure 1. Experimental apparatus 1, CO_2 gas tank; 2, Humidifying column; 3, Humidifying column; 4, Micro syringe (gas injection); 5, Micro syringe (liquid injection); 6, Capillary tubing; 7, Thin light beam source; 8, Photo transistor; 9, Turning cup; 10, Absorption column; 11, Solenoid valve; 12, Pressure transducer; 13, Camera platform; 14, Counter weight; 15, Motor; 16, Motor controller; 17 Camera; 18, Stroboscope; 19, Mirror; 20, Meter stick; 21 Narrow light slit (two of them); 22, Photo transistors (two); 23, Microswitch; 24, Flood lamp; 25, Bleed valve; 26, Pressure transducer indicator; 27, Magnetic sensor amplifier; 28, Digital voltmeter; 29, Slit-light control relay; 30, Variac; 31, DC power supply for camera motor; 32, Platform control circuitry; 33, Velocity measuring circuitry; 34, Digital counter; 35, 4-channel recorder.

Measurements of bubble velocity, bubble shape and instantaneous mass transfer rates, as well as streakline flow visualization, are all carried out near the mid-line of the column where flow transients and other effects are minimized.

The velocity of bubble rise was initially measured by simple multiple-image photography following Leal *et al.* (1971), and this approach was adequate for the dynamics experiments. However, in correlating mass-transfer data it was found that a more reproducible and reliable method was needed in order to minimize scatter. Hence, a simple system was designed in which bubble velocities could be measured automatically and accurately using a combination of two phototransistors with associated pencil-line light sources and an electronic counter. When the bubble passes the lower phototransistor, a pulse is generated which activates the electronic counter. A second pulse, generated by the second phototransistor, stops the counter which thus provides an accurate measure of the elapsed time between pulses. From this time, and the known distance between the phototransistors, the velocity of bubble rise may be calculated. The system is extremely reproducible provided that the bubble shape and motion does not exhibit any oscillating character, and the system is carefully aligned.

2. *Bubble formation and release mechanism*

Poor design of the bubble release mechanism has been one of the major factors in the lack of consistency between mass-transfer data obtained by different investigators. An example of the potential difficulties are wild oscillations of shape, or local turbulence, created during the release process which have contributed to an apparent age dependence of mass-transfer rates, cf. Deindorfer & Humphrey (1961).

There are two distinct types of bubble formation and release mechanisms which have been used extensively. For small bubbles almost all of the previous investigators used glass (metal) nozzles, orifices or hypodermic needles (cf. Haberman & Morton 1953). Larger ones were exclusively created by a turning cup (Peebles & Garber 1953; Leonard & Houghton 1963; Calderbank & Lochiel 1964; Leal *et al.* 1971). Despite criticism, the turning cup technique still remains the most reliable way of producing single large bubbles. Zieminski & Raymond (1968, 1971) used a capillary tube technique which was credited with yielding more reproducible results. With this method however, it was not possible to produce bubbles larger than 0.25 cm^3.

In the present work both the capillary tube and the turning cup are used for different ranges of bubble sizes. Figure 2 shows the capillary tube release mechanism in more detail. The capillary tube has a nominal diameter of 2 mm, but is enlarged to 4 mm at its upper end. CO_2 gas is introduced into the tube by a hypodermic needle and is pushed out by a micro syringe filled with the same liquid that is in the absorption column. The enlargement of the tube at its upper end allows the bubble to assume a form close to its final shape before it leaves the tube, thus minimizing initial oscillations in shape. With a smooth, slow release we have also found that the bubble path upward through the column is extremely reproducible, a critical prerequisite to accurate flow visualization. The turning cup mechanism used for large bubbles is not as reliable, but because of the relatively high viscosities of the test fluids, the initial disturbances do damp out relatively quickly.

3. *Mass-transfer measurements*

In order to determine the instantaneous rate of mass transfer from a bubble rising through a quiescent liquid, it is necessary to measure its instantaneous volume, surface area and pressure. All of the current methods use photographs to determine the surface area. However, they do differ in the method of measuring bubble volume. Two basic techniques have been employed. The simplest is to estimate the rate of change of bubble volume from the same photographs as are used to determine surface area. With care, this method can yield reasonable results provided the ambient liquid is quite viscous so that the bubble shape is simple and exhibits no oscillations. The alternative approach, which is particularly useful when the bubble shape is

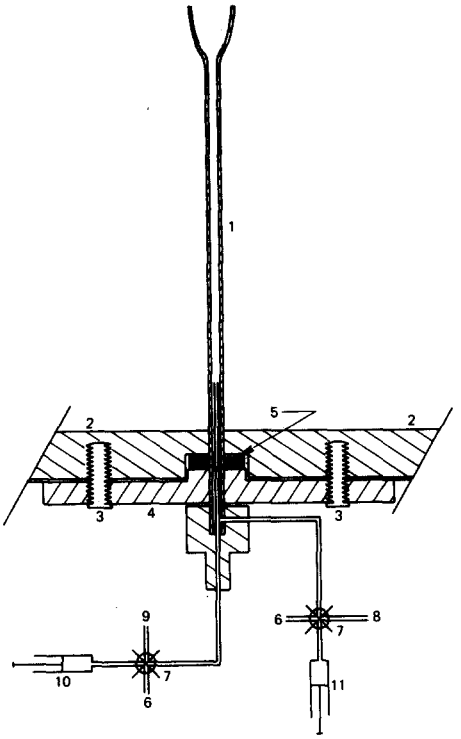

Figure 2. Bubble release mechanism. 1, Graduated capillary tube; 2, Bottom plate of the absorption column; 3, Screws to hold the seal plate; 4, Seal plate; 5, Gas jet; 6, Purge line; 7, 3-way valve; 8, Liquid reservoir line; 9, Carbon dioxide line; 10, Graduated gas syringe; 11, Liquid syringe.

neither simple nor steady, is to determine the change in bubble volume from an indirect measure of the space it occupies. A number of variations on this basic theme have been proposed. With the capillary method, the column is filled completely with liquid and the system is open to the atmosphere only through a small capillary tube. The change in bubble volume is correlated with the motion of the meniscus of the liquid in the capillary. The chief difficulty with this method is the delay in response of the capillary fluid due to viscous (viscoelastic) effects. A similar method, in spirit, is the constant-volume system used by Calderbank *et al.* (1970). Here the column is completely filled with liquid, closed to the atmosphere and the mass-transfer rate determined by measuring the (uniform) pressure inside the column. The bubble volume is, of course, *constant* assuming that the surrounding fluid is incompressible and the column rigid. Although we can clearly obtain an accurate measure of volume (and surface area) with this method, *the mass-transfer rate will be relevant, in general, only if the system for which the data are to be applied is also a completely closed and filled system.* Otherwise, and especially for viscoelastic liquids (see the discussion of the preceding section) the extensional flow induced by the change in bubble volume can produce significant differences in mass-transfer rates. Indeed, for small *Pe* numbers we have shown in a previous paper (Zana & Leal 1975) that the whole mass-transfer process can be controlled by the rheologically imposed restrictions on the maximum rate of bubble collapse. Even for large *Pe* the present experiments will show that the collapse process can play a fundamental, and in this limit, somewhat unexpected role in the mass-transfer process, giving measurably different rates of mass transfer depending upon whether or not the bubble volume is changing.

A second pressure related method which does not suffer from the disadvantages of Calderbank's method is the so-called airspace-pressure method in which changes in bubble volume are detected by measuring pressure (volume) changes in a small airspace which is left at the top of the column. Recently Garbarini & Chi Tien (1969) presented a comparative study of

the airspace-pressure and photographic methods. The basic conclusion was that the photographic method provided more reliable results when the bubbles travel in straight paths with no oscillations and have simple, regular shapes.

The column which we used can be operated in either the airspace-pressure or photographic modes. However, the ambient fluids used in the present study were all extremely viscous and/or elastic, and the bubble motions and shape were very smooth and regular. Hence, all of the mass-transfer data which we will describe in later sections were obtained using the simple photographic method.

The photographs required to determine bubble surface area and volume were obtained using a Bolex H-16 motion picture camera mounted on a well-balanced moveable platform which is driven by a motor with an electronic variable speed controller and which can be controlled manually to track the bubble. The recorder and the camera were turned on just before the bubble was released. The camera platform was activated by the bubble itself. To achieve this, a light guide which sends a thin flat beam of light through the column onto a phototransistor was mounted on the column right above the bubble release mechanism. When the beam of light was partially blocked by the passing bubble, a pulse was generated by the phototransistor, which was amplified by a logic circuit and fed to a relay to activate the motor controller.

In order to achieve constant and reproducible framing rates, the camera motor was run using a D.C. power supply. During each run the voltage input to the camera motor was accurately set to a value determined using a previously obtained calibration between framing rate and voltage. In addition, the framing rate was checked periodically by an electronic counter, as described below.

Illumination for the pictures was provided by two General Radio electronic stroboscopes which were mounted on the camera platform. The shutter of the camera was synchronized to the strobes by rotating a small magnet which is mounted on a shaft of the camera in front of a magnetic pick-up, amplifying the signal and using it to trigger the strobe once per frame. These signals are also counted by a digital counter for a short period of time in order to accurately determine the framing rate.

In reducing the mass-transfer data, the vertical position of the bubble relative to some reference level must be known. In addition, to obtain an accurate scale factor for use in determining bubble surface area (or volume), it is necessary to know the precise lateral position of the bubble relative to the camera. In experiments of other investigators, the vertical position has usually been determined by simply putting a meter stick on the column wall opposite the camera. However, this has the disadvantage of requiring a large depth of field in order to focus simultaneously on both the bubble and the meter stick. This necessitates placing the camera further from the column, thus reducing the image size of the bubble. In the present system we have employed a set of mirrors to produce a virtual image of the meter stick which is essentially coincident with the bubble path of rise, thus minimizing the required depth of field. The *lateral* position of the bubble was obtained from a second Polaroid picture taken at right angles to the movie. The Polaroid camera and necessary flood lights were automatically triggered by a microswitch and relay attached to the moving platform for the motion picture camera.

4. *Data reduction*

Depending on the velocity of rise, 500–1000 frames of film were used for each run. The location and the dimensions of the bubble were obtained from every fifth or sixth frame, and its age during ascent determined from the frame number and framing rate. The bubble volume and surface area were determined by direct measurement of the circumference and projected cross-sectional areas using the observed fact that the bubbles were axisymmetric in all cases. The latter measurement was carried out as follows. The frame to be analyzed was projected on to the 61×61 cm screen of a microfilm editor. The screen of the editor was furnished with a

hairline whose position from some preset position was proportional to a measurable voltage obtained from a potentiometer. The potentiometer signal was fed into a digital voltmeter which digitizes the signal and relays the information to an automated IBM card punch where it was reproduced for numerical analysis of the bubble area and volume. The measured projected distances are converted to actual length in the experiment by calibration using a photograph of a grid which was suspended in the test column at a distance from the camera which was equal to that of the bubble. The same grid was also used to determine the amount of length-scale distortion from the center of the film to the edges. No measurable distortion could be detected. For a typical data point, approx. 60–80 equally spaced points were measured around the bubble surface. Final values for surface area and volume were determined by a numerical integration.

D. MATERIALS

As we have noted earlier, the present study was intended to investigate the role of viscoelasticity on the dynamics and dissolution of single gas bubbles. Therefore, in designing the experiments an attempt was made to encompass a series of ambient fluids which range from Newtonion to strongly viscoelastic in their rheological behavior.

The Newtonian fluid used was an 89% (w/w) aqueous solution of glycerine. This specific concentration had previously been used by Calderbank *et al.* (1970) in their study of bubble dynamics and mass-transfer, and so was an extremely convenient choice for the present study.

The viscoelastic fluids which we used were water and water/glycerine solutions of the commercial coagulation polymer, Separan AP30. An increase in viscoelasticity can be most easily attained by either increasing the polymer concentration in solution, or by increasing the solvent viscosity (cf. Bruce & Schwarz 1969). In the present study the solutions in increasing order of viscoelasticity were 0.1%, 0.5% and 1% w/w solutions of Separan AP30 in water, and a solution of 0.523% (w/w) Separan AP30, 45.6% water and 53.9% glycerine.

The zero-shear viscosity, the density and the power-law index, n, for these materials is listed in table 1. As discussed in section B, we shall use the power-law parameter as a measure of the degree of thinning of the shear viscosity. In general, the density and the zero-shear viscosity for each solution was checked for two samples, one from the top of the absorption column and one from the bottom, before and after each set of experimental runs in order to check the uniformity and degree of constancy of the solutions in the column.

The properties listed in table 1 are all intrinsic parameters of the materials used. As we have noted in section B, it is necessary to consider the Weissenberg number and the Reynolds number in order to fully characterize the relative contributions of fluid elasticity. The latter parameters do not depend only on the intrinsic fluid properties, but also the deformation rate due to the flow, which may be estimated as the ratio of the characteristic velocity and length scales, $U/2R_{eq}$. The needed rheological data, namely, λ_1 as a function of shear rate, can be deduced from measurements of the primary normal stress difference, N_1, and the shear viscosity of the solutions as a function of the shear (deformation) rate, γ. For the aqueous Separan solutions, the required data can be obtained from Leal *et al.* (1971). The data for Separan AP30/water/glycerine is available in Hill (1969).

Table 1. Physical parameters of the solutions

Liquid (25°C)	$\eta_0(p)$	ρ(g/cm^3)	n
89% Aqueous solution of glycerine	1.80	1.234	1.0
0.1% AP30/H_2O	2.48	0.997	0.80 ± 0.10
0.5% AP30/H_2O	23.92	0.997	0.72 ± 0.05
1.0% AP30/H_2O	123.00	0.997	0.48 ± 0.02
0.523% AP30–45.6% H_2O–53.9% glycerine	280.00	1.138	0.28 ± 0.02

E. BUBBLE SHAPES

The main purpose of the present study was to assess the importance of the velocity transition on mass-transfer characteristics for single, soluble gas bubbles. With this objective in mind, a rather short range of bubble sizes was used, $0.18\,\text{cm} \leqslant R_{eq} \leqslant 0.42\,\text{cm}$, centered around the nominal critical radius for the transition, $R_{eq} \sim 0.3\,\text{cm}$, which was obtained by Leal *et al.* (1971). On the other hand, the present experiments do cover a reasonably broad spectrum of ambient rheological properties and include both bubbles of constant volume (air) and bubbles (CO_2) whose volume is decreasing as a result of mass transfer. Thus, we believe that it is worthwhile to present some of the data which we have obtained for bubble shape and terminal velocity in the present study.

We have noted in section B that the bubble shape should depend on the relative magnitudes of the Reynolds number, the Weissenberg number and the Weber number. Two distinct domains may be identified. For low values of the Reynolds number, $Re \ll 1$, the relative importance of shape deformation is measured by $(We/Re)Wb$. For high $Re \gg 1$, on the other hand, the shape would depend only on Wb.

For the range of bubble sizes which we have considered, the four viscoelastic solutions actually span a range of Reynolds number from approx. 10^{-3} to 10^{2}. The dependence of Reynolds number on bubble size (R_{eq}), for each solution, is listed in table 2. The 1% Separan/water and the Separan/water/glycerine solutions have $Re < 1$, while the 0.1% and 0.5% Separan/water solutions produce $Re > 1$ (with the exception of the three smallest bubble sizes in the latter case). Also shown in table 2 is the Weissenberg number as a function of bubble size in the four viscoelastic solutions.

Bubble shapes were determined from photographs in all four Separan solutions both for air bubbles of constant volume and for dissolving CO_2 bubbles. In the latter case the images used were instantaneous visualizations taken directly from a motion picture of the bubble motion. Significantly, in the low Re cases where inertia effects were not important, no differences could be detected in the bubble shape for a given volume between the dissolving and non-dissolving cases. This observation is consistent with the qualitative expectations from section B where it was suggested that the flow induced by the collapse process plays a secondary role in the instantaneous bubble dynamics, provided only that $Pe \gg 1$. In present experiments, $Pe = 0(10^{3} - 10^{6})$ in every case.

A pictorial representation of bubble shape as a function of bubble size for the four viscoelastic solutions is presented in figure 3. The effect of fluid elasticity on shape is most clearly seen for the 1% Separan/water and the Separan/glycerine/water solutions where the Reynolds number is small. It is well-known that the equilibrium shape for a Newtonian fluid in the low Reynolds number range is *spherical* for any value of the surface tension. Thus the deviations from sphericity in these two cases are due entirely to the non-Newtonian characteristics of the ambient fluid. It may be seen that the main qualitative effect is an elongation in the direction of motion into a prolate teardrop shape. A convenient measure of the degree of deformation is the bubble eccentricity, which we define as its maximum width divided by its maximum dimension in the direction of motion (i.e. $E > 1$ for all prolate shape). The measured eccentricities are listed for all four solutions in table 2. It may be noted, that none of the values for E differs much from unity, i.e. none of the bubbles is drastically nonspherical. This suggests that a linear combination of the parameters, Wb and $Wb(Wb/Re)$, may be useful in correlating the degree of deformation from a spherical shape (cf. discussion of section B). It should be recalled, however, that it is generally necessary to provide a second parameter, in addition to We, as a measure of non-Newtonian effects (such as shear-thinning) which are characterized as purely-viscous, rather than elastic. Thus, if a linear combination of Wb and $Wb(We/Re)$ is to be successful in correlating eccentricity, it is most likely for the highest concentration solution and for the glycerine/water/Separan solution which are most strongly

Table 2. *Re*, *We*, *Re*/*We* numbers and eccentricity vs bubble size

	0.1%				0.5%				1%				AP30-H_2O-Glyc			
R_{eq}	*Re*	*We*	*We*/*Re*	*E*	*Re*	*We*	*We*/*Re*	*E*	*Re*	*We*	*We*/*Re*	*E*	*Re*	*We*	*We*/*Re*	*E*
0.20	13.93	3.67	0.268	0.94	0.23	1.85	8.04	0.87	0.002	1.96	980.0	0.87	0.008	2.45	306.0	0.82
0.22	21.67	3.72	0.171	0.92	0.46	2.12	4.61	0.83	0.006	2.15	358.0	0.80	0.014	2.91	208.0	0.78
0.24	30.53	3.83	0.125	1.08	0.80	2.25	2.81	0.81	0.011	2.38	216.0	0.78	0.022	2.96	135.0	0.74
0.26	35.86	3.82	0.106	1.18	1.30	2.35	1.81	0.84	0.022	2.69	122.0	0.79	0.034	2.98	88.0	0.73
0.28	40.96	3.85	0.093	1.28	1.83	2.48	1.36	0.84	0.040	2.96	74.0	0.76	0.050	3.28	65.0	0.72
0.30	43.20	3.92	0.090	1.42	2.45	2.54	1.04	0.85	0.066	3.04	46.0	0.76	0.072	3.46	48.0	0.71
0.32	46.18	3.70	0.080	1.48	3.41	2.52	0.74	0.85	0.103	3.28	32.0	0.74	0.114	3.65	32.0	0.70
0.34	48.96	3.68	0.075	1.54	4.18	2.60	0.62	0.89	0.219	3.29	15.0	0.72	0.151	4.01	27.0	0.69
0.36	51.02	3.67	0.072	1.64	5.32	2.65	0.50	0.90	0.306	3.42	11.0	0.71	0.231	4.10	18.0	0.68
0.38	53.15	3.51	0.066	1.72	8.15	2.68	0.33	0.96	0.401	3.49	8.7	0.71	0.268	4.13	15.0	0.66
0.40	66.62	3.51	0.052	2.00	10.17	2.71	0.27	1.00	0.555	3.53	6.4	0.70	0.361	4.16	12.0	0.65

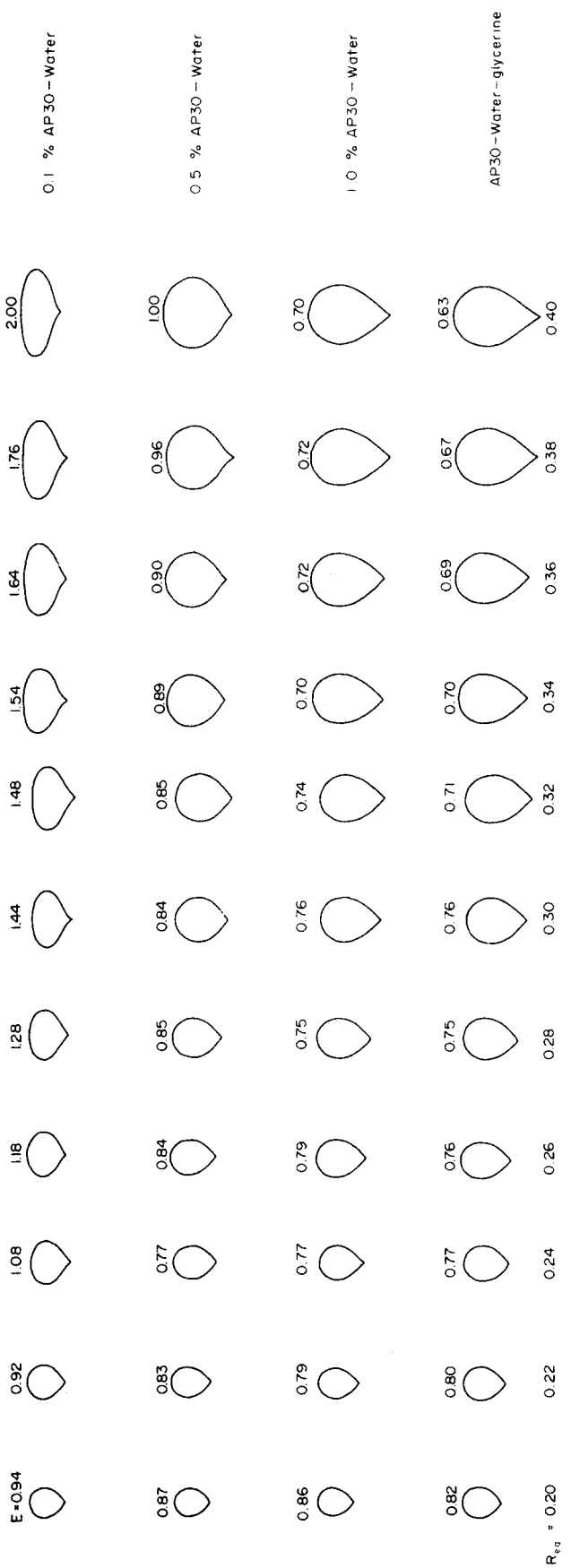

Figure 3. Bubble shape vs bubble size.

elastic. The most general linear form is

$$\hat{E} \equiv 1 - E = A_1 Wb + A_2 \left(\frac{Wb}{Re}\right) We = Wb\left[A_1 + A_2 \frac{We}{Re}\right]$$

and this suggests plotting $\hat{E}/Wb$ as a function of We/Re. It may be noted that this expression for $\hat{E}$ is identical with that derived rigorously by Wagner & Slattery (1972) for the limiting case $Re \ll 1$ and $We \ll 1$. The plot $\hat{E}/Wb$ vs We/Re is given in figure 4. The correlation between the 1% Separan/water and the Separan/water/Glycerine solutions is good, and the results are approximately linear for $We/Re < 30$, as suggested above. The results for the 0.5% Separan solution are also nearly linear, but *not* well correlated with those for the more viscoelastic solutions. The results for 0.1% Separan/water are not shown due to the great difference in the range of We/Re relative to the other cases, but are similar to the 0.5% solution in that they are more or less linear in We/Re, but poorly correlated with the results for the more viscoelastic solutions. We speculate that the poor correlation between the viscoelastically strong (1% and 0.523% in water/glycerine) and weak (0.1% and 0.5%) solutions is due to the relatively greater importance of the non-elastic, purely-viscous effects in the latter case, which are not well represented by We. The straight line $\hat{E}/Wb = -0.00852 + 00476\,(We/Re)$ which is shown in figure 4 is the best-fit line for the 1% Separan/water and 0.525% Separan/water/glycerine for $We/Re < 30$.

A qualitative rationale for the prolate shapes induced by fluid elasticity was suggested recently by Zana & Leal (1974). In brief, it was noted that a prolate shape is consistent with the general tendency of viscoelastic fluid flows to adopt configurations which reduce the likelihood of very large induced stress levels. In the motion of rigid bodies, it is known that the flow is streamlined (with a resulting reduction in the local rates of deformation), by increasing the length of the region fore and aft in which the flow is significantly influenced by the body (cf. Zana *et al.* 1975). For bubbles and drops, a similar effect can also be achieved by deformation of the bubble shape to an elongated form. This may provide at least a partial explanation for the prolate teardrop shapes which are actually observed. No detailed theory of bubble shape in viscoelastic systems is available.

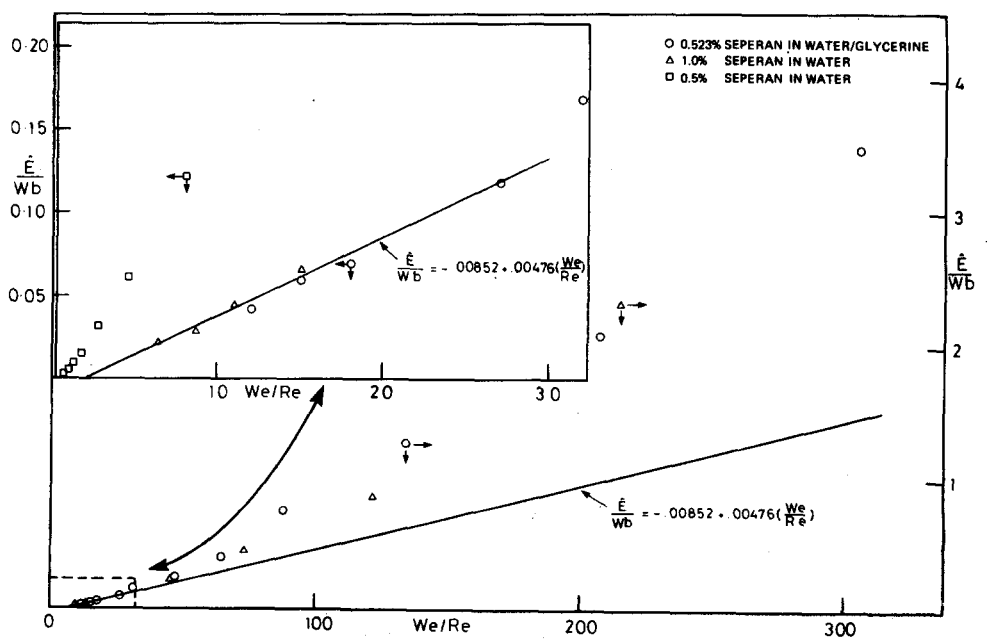

Figure 4. Bubble eccentricity vs Weissenberg number: Wb = Weber number, Re = Reynolds number, $\hat{E}$ = eccentricity, We = Weissenberg number.

F. BUBBLE RISE VELOCITIES

Instantaneous values were obtained for the velocity of rise for the CO_2 bubbles as a function of volume by careful frame-by-frame analysis of 16 mm motion pictures which were taken in conjunction with the mass transfer experiments. The framing rate for the velocity measurements was 16 frames/sec. The results for the 0.5% and 1% Separan/water solutions, and for the Separan/water/glycerine system are plotted in figures 5–7.† Also shown in these figures are measured values for the terminal velocity of air bubbles in the same materials. Finally, as a partial check on the accuracy of the present measurements, we have also included the data of Leal *et al.* (1971) for 0.5% and 1% Separan/water solutions. A discussion of the general characteristics of the velocity/volume relationship for bubbles in a viscoelastic fluid was presented by us in an earlier publication, Leal & Zana (1974). Included in that discussion are such features as the approach to the Davies–Taylor relationship for large bubbles, and the decreasing influence of elasticity in the small volume regime. Here we concentrate our attentions on the so-called velocity transition.

Examination of the data for air bubbles shows the existence of a large and discontinuous change in the terminal velocities in the 0.5% and 1% solutions, as well as the Separan/glycerine/water solution. The magnitude of the transition increases from a factor of about 4 for the 0.5% solution to a factor of 7 for the Separan/glycerine/water case, which is also the most viscoelastic. The bubble volume at transition is very nearly the same in all three cases. All of these features have been noted earlier, as indicated in the introduction to the present communication.

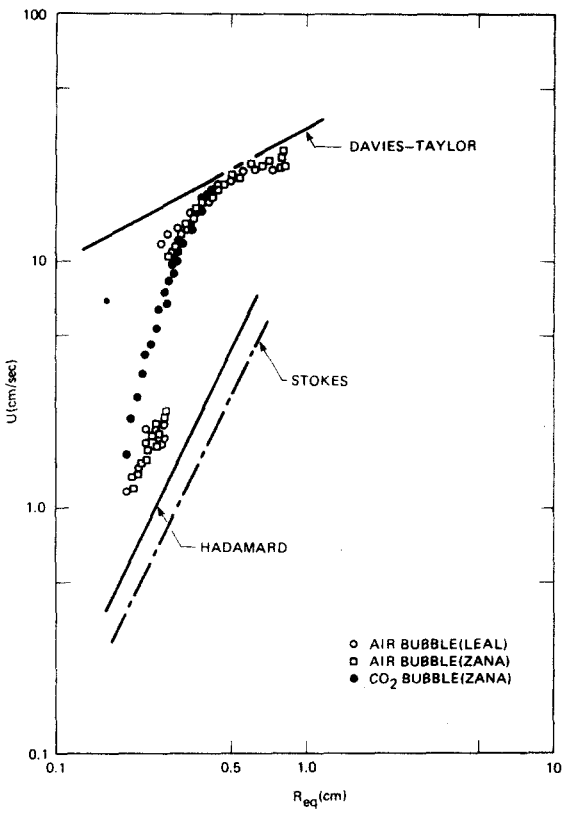

Figure 5. Bubble rise velocity vs size for 0.5% AP30/Weber solution: Davies & Taylor (1950); Leal *et al.* (1971); Zana, present work.

†Similar plots for the 89% glycerine/water solution and the 0.1% Separan/water solution may be found in Zana (1975). The data of Calderbank *et al.* in the glycerine/water system was included and shows excellent agreement with results from the present study.

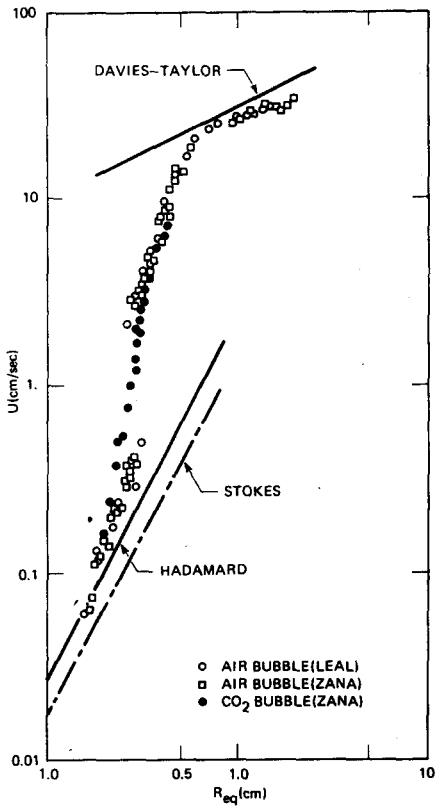

Figure 6.

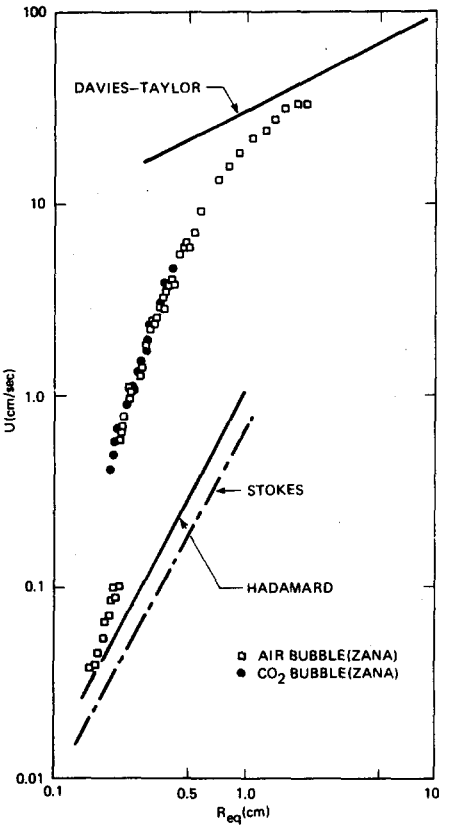

Figure 7.

Figure 6. Bubble rise velocity vs size for 1.0% AP30/water solution: Davies & Taylor (1950); Leal *et al.* (1971) Zana, present work.

Figure 7. Bubble rise velocity vs size for AP30/water/glycerine solution: Davies & Taylor (1950) Leal *et al.* (1971) Zana, present work.

The new and significant feature in the data of figures 5–7 is the fact that no discontinuity could be detected in the case of the dissolving CO_2 bubbles. For bubble volumes somewhat above and below the critical value, the measured instantaneous velocities for CO_2 bubbles are indistinguishable from the terminal velocities obtained for air bubbles of the same volume.† It is only in the immediate vicinity of the transition point that the data differ significantly. In each case, for volumes below the critical value, the velocities for the CO_2 bubbles are significantly larger than for the air bubbles. Since the air bubbles are known to behave as solid spheres before transition (cf. the comparison of bubble and solid sphere data in Leal *et al.* 1971), it may be surmised that the continuous decrease in volume of the CO_2 bubbles somehow leads to a change in the ability of the surface to sustain tangential stress, and thus to a smooth rather than abrupt transition in surface conditions, with an intermediate regime of partial internal circulation.

The difference in behavior of air and CO_2 bubbles can only be explained in terms of transient phenomena associated directly with the *boundary conditions* at the bubble surface. In particular, neither of the *bulk* hydrodynamic effects associated with the changing volume (i.e. transient velocities due to the changing buoyancy force, or the induced radial flow), could possibly account for the observed differences. Dimensional analysis, including mass transfer

†Terminal velocity data for air bubbles and instantaneous velocities for CO_2 bubbles were also indistinguishable in the glycerine/water and 0.1% Separan/water systems.

and associated transient hydrodynamic effects as described briefly in section B (and in detail in Zana & Leal 1975), shows that the induced radial velocity and the local fluid acceleration due to transients (i.e. $\mathrm{d}u/\mathrm{d}t$) are both of $0(Pe^{-1})$. Since Pe numbers in the present experiments ranged from $0(10^3)$ to $0(10^6)$, as noted previously, it is highly unlikely that these $0(Pe^{-1})$ effects could be significant. It may also be noted that the deviations in velocity, between the air and CO_2 bubbles, actually *increases* with bubble volume prior to transition, while Pe^{-1} *decreases*, thus providing further evidence that the $0(Pe^{-1})$ hydrodynamic effects are not significant. Finally, if either of these bulk hydrodynamic phenomena were significant, the deviations between the CO_2 and air bubbles would not be confined to the transition region, but would also be significant for larger and smaller bubbles where the data show no difference between the two cases. It is generally conceded (see the introduction), and the present experiments provide some further indirect evidence, that the abrupt "transition" in terminal velocities for air bubbles with $R_{eq} \sim 0.3$ cm occurs due to a change in effective surface conditions from no-slip for small bubbles to zero tangential stress for larger bubbles. As we have indicated in the introduction, previous studies have strongly suggested that the increase in magnitude of the velocity change from approx. 3/2 in the Newtonian case, to 0(5–10) in viscoelastic fluids, can be largely attributed to the changes in bulk rheological properties of the ambient fluid. The present experiments produce no information to contradict this hypothesis. Indeed, in table 3 we have tabulated the magnitude of the velocity transition from all of the available studies as a function of the power-law parameter n and the We. Reasonable correlation can be seen for both parameters. This not only provides some further evidence that the bulk rheology is important, but also shows that *both* (purely-viscous) shear-thinning and elastic effects play a significant role in establishing the magnitude of the transition, as suggested by Leal *et al.* (1971).

No physical explanation has ever been offered for the *abruptness* of the velocity transition compared to the Newtonian case. Clearly, however, any model which is proposed to account for the abruptness with bubbles of constant volume must also be able to accommodate a continuous change in the velocity when the bubble is undergoing a continuous decrease in volume. Two possibilities suggest themselves, which we shall first consider in light of the experimentally observed abrupt transition for constant volume air bubbles. We shall call the first the film model. The film model may be most easily explained as the formation on small bubbles of a membrane-like third (polymer) phase in which the polymer molecules are highly entangled, or otherwise interact in such a way as to afford the film some tensile strength. The abrupt transition is then envisioned as resulting from a rupture of the film, deriving from an instability for small disturbances (i.e. infinitesimal local variations in film properties) acted upon by the applied tangential shear stress from the fluid. One experimental observation which appears consistent with this suggestion is the fact that the quantity $(\mu U/a)$ at transition,

Table 3. Velocity transition

Solution	n	We	(Velocity increase factor) U_b/U_s
Newtonian	1.00	0	1.50
0.3% ET497 (Astarita & Apuzzo)	0.56	NA	2.22
0.25% J-100 (Astarita & Apuzzo)	0.55	NA	2.35
0.5% AP30–H_2O (this work)	0.72	1.85–2.54	4.00
1.0% Polyox (Calderbank *et al.*)	0.52	NA	4.15
1.0% AP30–H_2O (this work)	0.48	2.20–3.28	5.00
0.5% J-100 (Astarita & Apuzzo)	0.46	NA	5.55
0.7% ET497 (Astarita & Apuzzo)	0.44	NA	5.86
AP30–H_2O–glycerine	0.28	2.70–3.48	6.80

NA Not available

Under the column *We* number, first number corresponds to bubble *We* number just before transition, and the second number corresponds to the bubble *We* number just after the transition.

representing the magnitude of the shear stress, is essentially a constant. The only other work in the bubble dynamics literature which appears to be related to this concept of a bursting film was due to Griffith (1962) who reported that the paths of bubbles rising through glycerine containing oleic acid were sometimes made up of vertical rises separated by sudden lateral jumps. Griffith speculated that this jump stemmed from a non-symmetrical rupture of a film at the bubble surface. It is interesting to note that the existence of these lateral jumps was only reported for the oleic acid/glycerine system, and that oleic acid is a moderately long chain molecule, not unlike a polymer.

The second possible model for explaining the abruptness of the velocity transition is most conveniently called the surfactant model. In this case the polymer molecules are viewed as acting in the familar manner of more common surfactant materials (cf. the recent review by Harper 1972), with the no-slip condition for small bubbles arising due to the existence of flow-induced gradients of surfactant (and hence of surface tension) on the bubble surface. With this model the abruptness of the transition can only be explained as being an indirect result of its large magnitude. In the Newtonian case where the difference between the no-slip and zero-shear stress conditions is only a factor of approx. 3/2 in the terminal velocity, it is relatively easy to establish intermediate regimes of partial circulation as represented, for example, by the familiar Savic cap model (cf. Davis & Acrivos 1966). In the viscoelastic fluid, however, the magnitude of the velocity change associated with even a partially circulating condition is so large that the "cap" may simply not be able to exist in an intermediate state of partial coverage.

Although neither the film nor surfactant model has been subjected to any meaningful theoretical (or experimental) study in the present context, it is nevertheless appropriate to see whether either is capable of conceptual extension to the case of dissolving bubbles of constantly decreasing radius. Turning first to the film model, we can only say that it is difficult to see why a film which must be collapsing or folding onto itself (in view of the constant decrease in surface area) should be capable of allowing the appearance of partial internal circulation. The film model appears to us to be an "all or nothing model" in the sense that it can only allow complete circulation or complete no-slip conditions. Thus, from the point of view of generalization to the continuous velocity spectra of a collapsing bubble, the film model seems particularly deficient. In passing, it may also be noted that the mass-transfer data to be presented in the next section shows no sign of inhibition prior to transition, relative to the rates for a "clean" surface, as might be expected if one took the third-phase film concept seriously. In contrast to the film model, the surfactant model does appear to offer a possible mechanistic explanation for the observations with both constant volume and collapsing bubbles. With large concentrations of surfactant (polymer) in the bulk fluid (as we have in the present experiments) it is generally believed that at steady state the surfactant material takes on a surface concentration distribution with a minimum value at the front stagnation point and maximum (saturation) values at and near the back. The dynamics of establishing this equilibrium configuration are complex, involving bulk diffusion and convection of the polymer molecules to and from the bubble surface, absorption (and desorption) onto or off of the surface, and advection/diffusion of the polymer molecules on the surface itself. For large surfactant molecules it is generally believed that a time scale of 0(1 min) is required to attain a steady state surface concentration distribution (cf. Griffith 1962). When the bubble is collapsing, the available surface area is constantly decreasing, and so the distribution of surfactant (polymer) on the surface must be continuously readjusting itself. In particular, as the local surface area is decreased, surface concentrations of surfactant (polymer) near the rear of the bubble will exceed the equilibrium saturation value and desorption of surfactant (polymer) molecules must occur. At the same time a redistribution on the surface must occur toward a new equilibrium configuration. A little thought will show that this redistribution must correspond to a net advection of the molecules (and thus of the surface itself) from front to back, i.e. to a crude

approximation of the *partial* slip condition at the interface. Since the characteristic collapse time for the bubbles in the present experiments (equal to a $/\mathbf{U}\cdot\mathbf{n})$) is considerably shorter (i.e. ~ 10 s) than the time scales of 0(1 min) for complete establishment of a new steady state, it may be suggested that the surface concentration distribution will always be in a transient state, thus leading to a surface which is continually "flowing" from front to back in pursuit of a new equilibrium configuration. In this latter "model" the collapse process and especially its *rate* of occurrence plays a critical role as the experiments suggest that it should.

G. MASS TRANSFER

We now turn to the main objective of the present work, the experimental measurement of mass transfer rates from single gas bubbles in viscoelastic ambient fluids. Of particular interest is the correspondence between rates of mass transfer and the sharp (but continuous) change in bubble velocity near the critical transition volume.

The common practice among experimentalists has been to correlate mass transfer data in terms of the liquid phase mass transfer coefficient, k_L, defined as

$$k_L = -\frac{\mathrm{d}n/\mathrm{d}t}{A(c^* - c_L)}.$$

Here A is the surface area of the bubble available for mass transfer, $\mathrm{d}n/\mathrm{d}t$ the rate of change of bubble mass, and c^* and c_L the CO_2 concentrations at the gas–liquid interface and in the bulk of the solution, respectively. More convenient for theoretical work are the dimensionless Sherwood and Peclet numbers.

$$Pe \equiv \frac{2R_{eq}U}{D_L}; \qquad Sh \equiv \frac{2R_{eq}k_L}{D_L}$$

where R_{eq} is the equivalent radius, U, the instantaneous velocity of rise, and D_L the liquid phase diffusion coefficient. Whether k_L or Sh is used, however, experimental determination of the rate of mass transfer requires measurement of

i. the instantaneous bubble surface area;
ii. the instantaneous bubble volume;
iii. the rate of change of bubble volume;
iv. the instantaneous vertical position of the bubble relative to the surface of the liquid.

In addition, calculation of the Peclet number requires

v. the instantaneous rise velocity.

The quantities ii and iii are used to determine the rate of change of the moles of gas, $\mathrm{d}n/\mathrm{d}t$, through the perfect gas law, $PV = nRT$, and the instantaneous internal pressure, which is calculated using iv. It is assumed in this calculation that the mass transfer process occurs sufficiently slowly that the internal pressure is always in equilibrium with the local hydrostatic pressure. The quantity c^* is calculated from the internal pressure using Henry's law. The Henry's law constant is assumed to be the same as for pure water or water/glycerine. Measurements by Calderbank (1970) and others indicate that this is quite a good approximation at the relatively low polymer concentrations considered here.

Among the experimentally measured quantities, the most difficult to determine accurately are the bubble surface area and volume. As we have noted earlier, these quantities were determined by numerical integration using a cross-sectional photograph of the bubble, and the assumption of axisymmetry (a good assumption in our system). Most previous studies have used a more crude method in which volume and area are calculated from the measured "major" axes of the bubble assuming its shape to be spheroidal. In the Newtonian case such a procedure may yield quite accurate results, especially for small deviations from sphericity. However, in

the viscoelastic fluids considered here the bubble shape is clearly not spheroidal so that an approximation of this type could lead to considerable errors in the calculated mass-transfer rates. Calderbank *et al.* (1970) used a modified version of the spheroidal geometry approximation. To estimate the magnitude of error introduced by the spheroid assumption we calculated the ratio of the directly measured (exact) to approximated surface areas. The calculated approximate values were consistently larger than the exact measured ones; however, the errors are smaller than might be expected, approx. 8 to 10%. In addition, the "exact" values are within 5–20% of the area of a sphere with the same volume. In spite of these surprisingly reasonable approximate results we shall use the "exact" measured values of surface area in the present work.

Before discussing the experimental data on bubble mass transfer rates, it is useful to recall the various theoretical results which are available. We consider here only those expressions which are relevant to $Pe \gg 1$. For $Re \ll 1$, and a Newtonian ambient fluid, Levich (1962) showed that

$$Sh = 0.991\ Pe^{1/3} \qquad (Pe \gg 1,\ Re \ll 1) \qquad [1]$$

for a rigid sphere, and

$$Sh = 0.65\ Pe^{1/2} \qquad (Pe \gg 1,\ Re \ll 1) \qquad [2]$$

for a spherical bubble with free circulation. For a circulating sphere at large Reynolds number, Boussinesq (1905) used the pontential flow solution for the velocity field to obtain

$$Sh = 1.13\ Pe^{1/2} \qquad (Pe \gg 1,\ Re \gg 1). \qquad [3]$$

The latter result is, of course, not restricted to a Newtonian fluid. As we have noted earlier, if Re is sufficiently large that the inertia terms in the equation of motion are dominant over viscous or elastic contributions, the velocity field will be the potential flow solution *independent* of the bulk rheological properties. Thus, for sufficiently large bubbles in either the Newtonian or viscoelastic fluids, one would expect to find data correlation according to [3], provided the bubble shape remained spherical. Even for nonspherical shapes, however, the general result

$$Sh = cPe^{1/2} \qquad [4]$$

will hold, with the constant c depending on bubble shape. No comprehensive theory of bubble mass transfer in viscoelastic fluids is available at low Reynolds numbers. The reason is simply that no comprehensive theory has yet been developed for the velocity field and bubble dynamics. The only results available are (like the velocity field modifications) limited to small deviations from a Newtonian fluid. For a power-law fluid with $|n-1| \ll 1$, Hirose & Moo-Young (1969) have shown that the Sherwood number for a circulating bubble in the creeping flow regime is given by

$$Sh = 0.65\left[1 - \frac{4n(n-1)}{2n+1}\right]^{1/2} Pe^{1/2}. \qquad (Re \ll 1,\ Pe \gg 1) \qquad [5]$$

More recently, Moo-Young & Hirose (1972) considered the small We limit for a Maxwell fluid in the creeping flow regime to show

$$Sh = 0.65\{1 + 0.16\ We^2\}Pe^{1/2} \qquad (Re \ll 1,\ Pe \gg 1) \qquad [6]$$

for $We \ll 1$. Neither [5] nor [6] is directly applicable to the strongly non-Newtonian solutions

used in the present study in view of the restrictions on $|n-1|$ and *We*. However, they can at least be examined for qualitative trends which may be useful outside their strict range of validity. In this sense, [5] predicts an enhancement in the mass transfer rate over its Newtonian value as a result of shear dependence of viscosity. Furthermore, the enhancement increases monotonically with decrease of the flow index, *n*. The predictions of [6] are similar to those of [5]. It shows an increase in the mass-transfer rate with increasing viscoelasticity, i.e. with *We* number.

Measured mass transfer rates for CO_2 bubbles in 89% glycerine–11% water solution are shown in figure 8. Also shown in figure 8 is the experimental data of Calderbank *et al.* for the same system. The agreement between the two is excellent. This is significant, because the Calderbank *et al.* (1970) mass transfer data were obtained in a "closed" system where the bubble volume remains constant during its rise through the column. We have noted previously, in section C, that this could lead to significant differences in mass transfer rate when compared to an "open" system where the bubble volume is allowed to vary. The difference between an "open" and a "closed" system could be important for cases in which the flow induced by the interface motion is significant compared to the translational motion of the bubble. In glycerine/water solution the mass transfer rates are very small due to extremely small liquid phase diffusivity, D_L, and hence the interface motion is negligibly small. As a result, in the absence of significant transient effects associated with the interface itself (as seem to occur in the viscoelastic case—see previous section), the "closed" and "open" systems are expected to yield comparable results in the glycerine/water solution. For completeness, we note that the agreement between the rise velocities of air bubbles and CO_2 bubbles measured in this work, and CO_2 bubbles obtained by Calderbank *et al.* (1970) is excellent (cf. figure 6 of Zana 1975). We have also plotted the theoretical expressions [1–3] in figure 8. Agreement between the data and [3] is good for the larger bubbles where *Re* is moderate.

The mass transfer data for the 0.1, 0.5, 1.0% Separan AP30/water solutions and the Separan/water/glycerine solution are shown in figure 9–12, plotted as *Sh* against *Pe*. Also shown in each figure are the most appropriate of the theoretical expressions [1–5].

Initially, a point of surprise regarding these data is the fact that they appear smooth over the

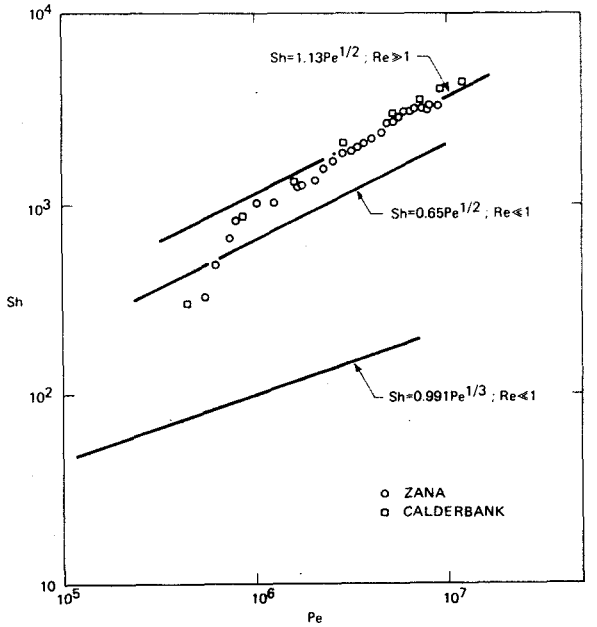

Figure 8. *Sh* Number vs *Pe* number for 89% glycerine/water solution: Zana, present work; Calderbank *et al.* (1970).

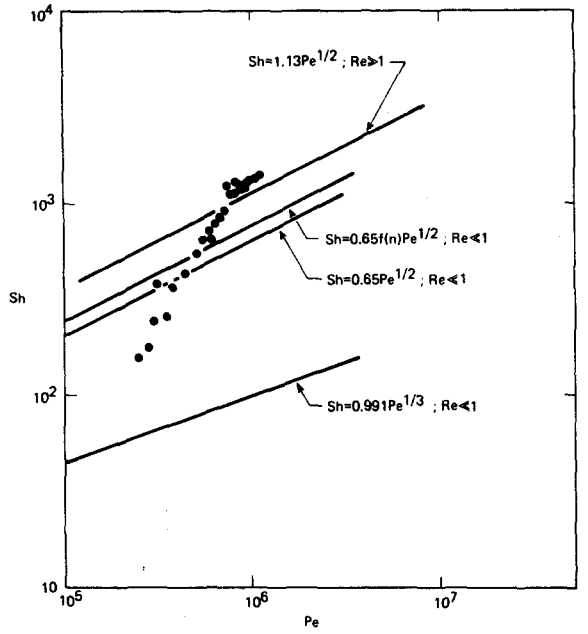

Figure 9. *Sh* Number vs *Pe* number for 0.1% AP30/water solution.

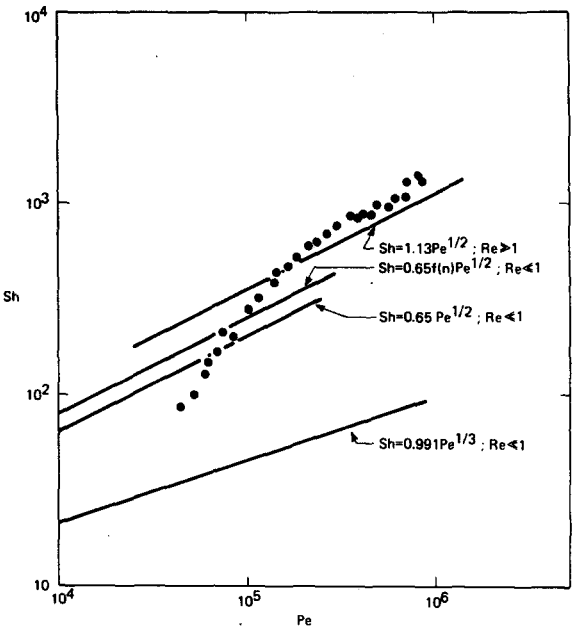

Figure 10. *Sh* Number vs *Pe* number for 0.5% AP30/water solution.

whole range of *Pe*, with no apparent region of rapid (though continuous) increase as found in the velocity data of the preceding section. It is thus important to point out that a corresponding transition actually does occur, which would be evident if *Sh* were plotted as a function of R_{eq} instead of *Pe*. *Pe* involves *U* and so itself increases sharply in the transition region. This causes the corresponding sharp increase in *Sh* to be spread out horizontally, thus producing the smooth curves of figures 9–12.

For all of the systems studied here $Pe \geq 10^3$, so that one of the restrictions of [1–6] is automatically satisfied. As we have noted in section D, the four viscoelastic solutions fall into two groups with respect to *Re*. In the higher *Re* group, glycerine/water and 0.5% Separan/water

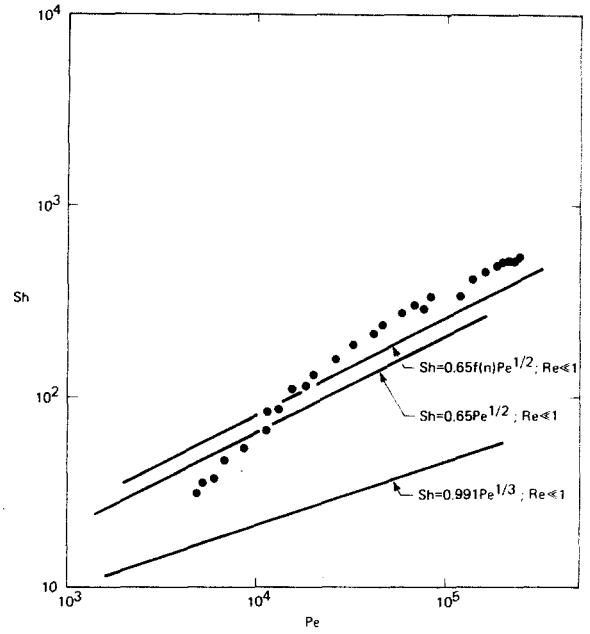

Figure 11. *Sh* Number vs *Pe* number for 1.0% AP30/water solution.

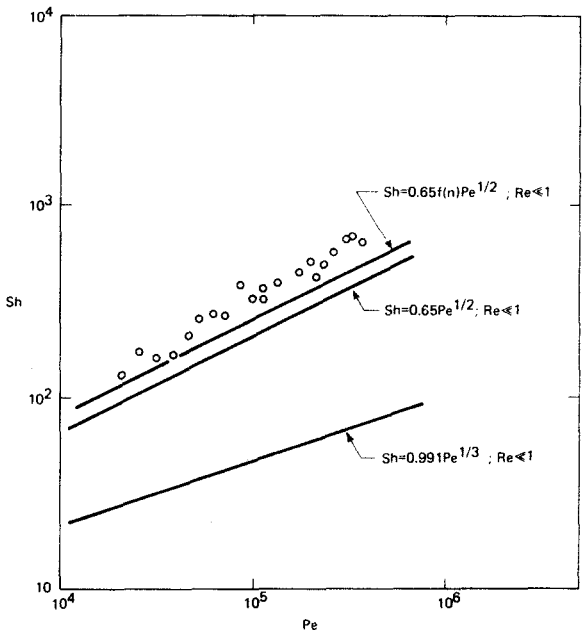

Figure 12. *Sh* Number vs *Pe* number for AP30/water/glycerine solution.

have Reynolds numbers ranging from ~ 3 to 20, while 0.1% Separan/water ranges from ~ 15 to 70. Our comparison of the experimental data for the Newtonian glycerine/water system with [3] showed good agreement for the larger bubble sizes where the *Re* is largest. It should be noted, however, that the bubble shapes differed substantially from spherical so that this agreement may be fortuitous. Indeed, for the two comparable viscoelastic systems (0.1 and 0.5%), the data cross over the high Reynolds number theoretical expression to values which are 10–13% larger in the 0.1% solution, and 22–25% greater for 0.5% Separan/water. We shall discuss this apparent enhancement in mass transfer rates in more detail later in this section. However, we may note that we believe the enhancement to be a genuine product of the viscoelasticity and shear-thinning properties of the fluid.

For the 1% AP30/glycerine/water and AP30/glycerine/water solutions, Re varies from 10^{-3} to 0.5, and the experimental data must be compared with the low Reynolds number theories, as indicated in figures 11 and 12. For the 1% AP30/water solution, the data start between the theoretical curves for solid and freely circulating spheres, and increase to values, for the largest bubbles, which are substantially greater than either the Newtonian or power-law expressions [2] and [5]. The intermediate values obtained for the smallest bubbles are actually consistent with the velocity data of the preceding section. It was noted there that the velocities for the CO_2 bubbles in viscoelastic solutions are always greater than the corresponding velocities of air bubbles for $R_{eq} < R_{\text{critical}}$, and it was argued that this increase could be due to a partial internal circulation for the CO_2 bubbles. The mass transfer data are consistent with this hypothesized existence of partial circulation, since they lie halfway between the no-slip and freely circulating theoretical predictions. It is also significant, as we pointed out in the previous section, that the polymer molecules at the bubble surface do not appear to directly inhibit CO_2 transfer to the surrounding fluid. Turning to figure 12, it may be noted that the mass-transfer data for AP30/water/glycerine lie strictly above the predictions of [2] and [5]. This is again consistent with the velocity data for CO_2 bubbles in the same solution, figure 7, which show that the smallest bubbles represented in the mass transfer data ($R_{eq} = 0.20$ cm) have a velocity very close to the velocity of the fully circulating, post-transition air bubbles.

Table 4 shows the percentage increase in experimental mass transfer rates over the predicted Newtonian values both for the four viscoelastic solutions used in the present study and also for all other available mass transfer data in non-Newtonian fluids. Also listed are Re, n, and either We or We/Re, depending upon where $Re < 1$ or $Re > 1$, respectively. Finally, we have also listed the percentage increase above the prediction of the $|n-1| \ll 1$ power-law theory for those cases where $Re < 1$. It will be noted that the various cases are listed in order of decreasing power-law index, n.

Turning first to the four cases studied in the present work, it may be seen that the 10–13% and 22–25% increases for 0.1 and 0.5% AP30/water correlate well with an increasing level both of shear-thinning (n) and of effective fluid elasticity (We/Re). Likewise for 1% AP30/water and AP30/water/glycerine where n is further decreased, the increase in mass transfer rate above the Newtonian value is also further increased from 56 to 60 and 60 to 65%, respectively, and ordered with respect both to n and to the appropriate measure of elasticity, We, for the low Re cases.

Considering all of the cases which are listed, we may note

(i) The degree of increase in mass transfer rates correlates well with the power-law index, n, for all cases except the 0.14% Carbopol solution studied by Hirose & Moo-Young (1969). We believe that the lack of correlation in this one case is extremely significant since all of the solutions listed are fully viscoelastic except for Carbopol which is a shear-thinning, purely-viscous liquid. The implication is that the fully-viscoelastic values of mass-transfer rate represent the additive contribution of shear-thinning and separate elastic effects. In other words, one cannot, in general, expect correlation of the enhancement of mass transfer rates and n, without also taking into account the appropriate measure of importance of elastic effects. For all solutions except 0.1 and 0.5% AP30/water, this, is We. For these two cases, one must use (We/Re) as the measure of elasticity since the Reynolds numbers of the bubble motion are moderate to large.

(ii) The increase in mass transfer rates is greater than predicted by the power-law model of Hirose & Moo-Young (1969). Although this theory is strictly valid only for $|n-1| \ll 1$, it was suggested by Calderbank *et al.* (1970) that the experimental data even in strongly viscoelastic liquids could be predicted by using the power-law theory with measured values of n. Since the power-law model represents only the effect of a shear-thinning viscosity, it was thus suggested that the influence of elasticity was of negligible importance. This result is, of course, surprising in view of the potential influence of elasticity on the flow patterns,

Table 4. Comparison of experimental mass transfer rates with predictions of Newtonian theory

Solution	Re	n	We	We/Re	% Increase in Sh over the Newtonian value (experimental)	% Increase over power-law model [23]
2.5%CMC–H_2O (Hirose & Moo-Young)	$Re < 1$	0.86	0.50	Not applicable	9–12%	1–4%
0.1% AP30–H_2O (this work)	40–70	0.85	Not applicable	0.08	10–13%	Not applicable
0.5% AP30–H_2O (this work)	5–10	0.72	Not applicable	0.27	22.25%	Not applicable
1.0% HEC (Hirose & Moo-Young)	$Re < 1$	0.70	0.80	Not applicable	25.30%	9–14%
1.0% Polyox (Calderbank *et al.*)	Not available	0.54	Not available	Not available	40–45%	15–20%
1.0% AP30–H_2O (this work)	0.1–0.4	0.48	3.40	Not applicable	56–60%	35–39%
0.14% Carbopol (Hirose & Moo-Young)	$Re < 2$	0.34	0.00	Not applicable	30–35%	3–5%
AP30–H_2O–Glycerine (this work)	0.07–0.4	0.28	3.80	Not applicable	60–65%	37–42%

and is also at odds with the prediction for small *We* given by [6]. The present experimental results show that increases of as much as 25% can be obtained above the power-law theory when the ambient fluid is fully viscoelastic. Furthermore, these increases correlate strongly with the relevant measure of the fluid's elasticity, i.e. *We* or *We*/*Re* in every case.

4. CONCLUSIONS

(i) It is shown through dimensional analysis and examination of experimental data that the effect of fluid elasticity on the rise velocities and mass transfer rates can be correlated in terms n and the *We* number when $Re \ll 1$, and n and (We/Re) when $Re \gg 1$.

(ii) It is found experimentally that the effect of elasticity on the bubble shape is to stretch it along the streamlines to a prolate teardrop shape. This shape of bubble is consistent with the streamline pictures of a viscoelastic liquid moving past a solid sphere.

(iii) It is shown for the first time that the discontinuous increase in velocity of rise corresponding to a change from rigid to free surface conditions only occurs for non-dissolving (constant volume) air bubbles, and that the transition is smooth for dissolving (varying volume) CO_2 bubbles. Two qualitative models relating to the abruptness of the velocity transition for air bubbles, are discussed in terms of the observed difference between constant volume and collapsing bubbles.
abruptness of the velocity transition for air bubbles, are discussed in terms of the observed difference between constant volume and collapsing bubbles.

(iv) Mass transfer rates were measured for one Newtonian and four visco-elastic liquids. The mass-transfer rates are found to be significantly enhanced as a result of viscoelasticity. The increase in mass transfer rates over the corresponding Newtonian values are found to increase with increasing shear dependence of viscosity and/or elasticity. However, it is shown that the shear dependence of viscosity cannot alone account for the large increase in mass transfer rates, and hence that elasticity has to be included in any successful analysis of the mass transfer data for viscoelastic fluids.

REFERENCES

ASTARITA, G. & APUZZO, G. 1965 Motion of gas bubbles in non-Newtonian liquids. *A.I.Ch.E.Jl.* **11**, 815–820.

BOUSSINESQ, J. 1905 *J. Math. Pure Appl., Ser.* VI, **1**, 285–332.

BRUCE & SCHWARZ, 1969 Rheological properties of ionic and nonionic polyacrylamide solutiond. *J. Polym. Sci. A*-2, **7**, 909–927.

CALDERBANK, P. H., JOHNSON, D. S. L. & LOUDON J. 1970 Mechanics and mass transfer of single bubbles in free rise through some Newtonian and non-Newtonian liquids. *Chem. Engng Sci.* **25**, 235–256.

DAVIES, R. M. & TAYLOR, G. I. 1950 The mechanics of large bubbles rising through extended liquids and through liquids in tubes. *Proc. R. Soc.* **A200**, 375–390.

DAVIES, R. & ACRIVOS, A. 1966 The influence of surfactants on the creeping motion of bubbles. *Chem. Engng Sci.* **21**, 681–685.

DEINDORFER, F. H. & HUMPHREY, A. E. 1961 Mass transfer from individual gas bubbles. *IEC Fundamentals* **53**, 755–759.

GARBARINI, G. R. & CHI TIEN 1969 Mass transfer from single gas bubbles—a comparative study on experimental methods. *Can. J. Chem. Engng* **47**, 35–41.

GRIFFITH, R. M. 1962 The effect of surfactants on the terminal velocity of drops and bubbles. *Chem. Engng Sci.* **17**, 1057–1070.

HABERMANN, W. L. & MORTON, R. K. 1956 An experimental study of bubbles moving in liquids. *Trans. Am. Inst. Civil Engrs.* **121**, 227–252.

HARPER, J. F. 1972 The motion of bubbles and drops through liquids. *Ad. Appl. Mech.* **12**, 59–129.

HILL, C. 1969 Ph.D. Dissertation. University of Wisconsin.

HIROSE, T. & MOO-YOUNG, M. 1969 Bubble drag and mass transfer in non-Newtonian fluids: Creeping flow with power-law fluids. *Can. J. Chem. Engng* **47**, 265–267.

LEAL, L. G., SKOOG, J. & ACRIVOS, A. 1971 On the motion of gas bubbles in a viscoelastic liquid. *Can. J. Chem. Engng* **49**, 569–575.

LEONARD, T. H. & HOUGHTON, G. 1963 Mass transfer and velocity of rise phenomena for single bubbles. *Chem. Engng Sci.* **18**, 133–142.

LESLIE, F. M. 1961 The slow flow of a viscoelastic liquid past a sphere. *Q. J. Mech. Appl. Math.* **14**, 36–48.

LEVICH, V. G. 1962 *Physiochemical Hydrodynamics*. Prentice Hall, Englewood Cliffs, NJ.

MOO-YOUNG & HIROSE 1972 Bubble mass transfer in creeping-flow viscoelastic fluids. *Can. J. Chem. Engng* **50**, 128–130.

OLDROYD, J. G. 1958 Non-Newtonian effects in steady motion of some idealized elastico-viscous liquids. *Proc. R. Soc.* **A245**, 278–297.

PEEBLES, F. N. & GARBER, H. Y. 1953 Studies on the motion of gas bubbles in liquids. *Chem. Engng Prog.* **49**, 88–97.

RAYMOND, D. R. & ZIEMINSKI, S. A. 1971 Mass transfer and drag coefficients of bubbles rising in dilute aqueous solutions. *A.I.Ch.E.Jl.* **17**, 57–65.

WAGNER, G. & SLATTERY, J. 1971 Slow flow of a non-Newtonian fluid past a droplet. *A.I.Ch.E.Jl.* **17**, 1198–1207.

ZANA, E. & LEAL, L. G. 1974 The dynamics of bubbles and drops in a visco-elastic fluid. *Proceedings of the International Colloquim on Drops and Bubbles* (Edited by COLLINS, PLESSET and SAFFREN) Vol. II.

ZANA, E. 1975 Ph.D. Dissertation. California Institute of Technology.

ZANA, E. & LEAL, L. G. 1975 Dissolution of a stationary gas bubble in a quiescent, viscoelastic liquid. *IEC Fundamentals* **14**, 175–182.

ZANA, E., TIEFENBRUCK, G. & LEAL, L. G. 1975 A note on the creeping motion of viscoelastic fluid past a sphere. *Rheol. Acta* **14**, 891–898.

ZIEMINSKI, S. A. & RAYMOND, D. R. 1968 Experimental study of the behavior of single bubbles. *Chem. Engng Sci.* **23**, 17–28.